

1 Evaluating the seismic behaviour of rammed earth buildings from 2 Portugal: from simple tools to advanced approaches

3 Rui A. Silva¹, Nuno Mendes², Daniel V. Oliveira³, Antonio Romanazzi⁴, Oriol Domínguez-Martínez⁵, Tiago
4 Miranda⁶

5 ¹⁻⁴ *ISISE, University of Minho, Guimarães, Portugal*

6 ⁵ *Terrachidia Association, Madrid, Spain*

7 ⁶ *ISISE & IB-S, University of Minho, Guimarães, Portugal*

8 **Abstract:**

9 Despite the use of rammed earth became marginal in the second half of the past century, Portugal still holds an
10 important built heritage. Recently, a growing use of rammed earth has been observed in modern constructions,
11 but it is putting aside the roots of traditional rammed earth construction. The seismic behaviour of rammed earth
12 buildings is still insufficiently comprehended, constituting a matter of great concern, since most of the traditional
13 dwellings are built on regions with important seismic hazard. Moreover, the complex architecture of modern
14 rammed earth buildings is expected to make their seismic behaviour even more fragile. This paper intends to
15 provide a better comprehension on the seismic behaviour of rammed earth constructions from Portugal. For this
16 purpose, twenty traditional dwellings were evaluated on the basis of a simplified approach, while a modern
17 construction was investigated by means of destructive and non-destructive testing approaches. The main findings
18 of these approaches are discussed in detail, but it can be highlighted that the architectural features of traditional
19 rammed earth buildings benefit their seismic behaviour, while the complex architecture of modern rammed earth
20 buildings demands using advanced engineering tools for their seismic assessment.

¹PhD, Post-doc researcher, ISISE, University of Minho, Department of Civil Engineering, Azurém, P-4800-058 Guimarães, Portugal.

Phone: +351 253 510 200, fax: +351 253 510 217, email: ruisilva@civil.uminho.pt

²PhD, Post-doc researcher, ISISE, University of Minho, Department of Civil Engineering, Azurém, P-4800-058 Guimarães, Portugal.

Phone: +351 253 510 200, fax: +351 253 510 217, email: nunomendes@civil.uminho.pt

³PhD, Associate professor, ISISE, University of Minho, Department of Civil Engineering, Azurém, P-4800-058 Guimarães, Portugal. Phone:

+351 253 510 200, fax: +351 253 510 217, email: danvco@civil.uminho.pt

⁴PhD student, ISISE, University of Minho, Department of Civil Engineering, Azurém, P-4800-058 Guimarães, Portugal. Phone:

+351 253 510 200, fax: +351 253 510 217, email: aromanazzi89@gmail.com

⁵Cofounder, Terrachidia Association, Madrid, Spain, email: oriol.arq@gmail.com

⁶PhD, Assistant Professor, ISISE & IB-S, University of Minho, Department of Civil Engineering, Azurém, P-4800-058 Guimarães, Portugal.

Phone: +351 253 510 200, fax: +351 253 510 217, email: tmiranda@civil.uminho.pt

21 **Keywords:** Rammed earth, seismic behaviour, simplified indexes, kinematic approach, mechanical
22 characterisation, dynamic identification, sonic tests, model updating.

23 **Highlights:**

- 24 - The seismic behaviour of rammed earth buildings was investigated;
- 25 - Traditional dwellings were evaluated by means of a simplified approach;
- 26 - Destructive and non-destructive testing was used for a modern building;
- 27 - The parameters affecting the seismic behaviour are discussed.

28

29 1. INTRODUCTION

30 Raw earth is known as a building material used for several thousands of years in many regions of the World. The
31 oldest use of this material is evidenced by archaeological excavations of the first permanent dwellings in
32 Southwest Asia, dating back to 10 000 BC [1]. The continuous use of raw earth resulted in several building
33 techniques, among which the most widespread are adobe masonry and rammed earth [2]. Generally speaking,
34 adobes are sundried mud bricks, typically layered with earth mortar to build walls, arches, vaults and domes [3].
35 In turn, building in rammed earth consists in compacting moistened earth inside a formwork to erect walls. The
36 formwork constitutes a key element within the definition of this technique, where traditional rammed earth walls
37 are mainly built by means of a crawling formwork made of timber [4]. This type of formwork is constituted by
38 different elements that allow easy mounting, removal and reuse.

39 A traditional rammed earth wall is formed by several large-dimension blocks composed by compacted layers of
40 earth. The formwork is supported directly on the wall and it is moved horizontally after completion of each
41 block. After conclusion of a lift, the formwork is moved upwards and mounted with mismatched vertical joints,
42 and then the process is repeated until the desired height of the wall is achieved. A formwork externally supported
43 can also be used to build in rammed earth, but it implies assembling a scaffolding structure [5]. The use of this
44 type of formwork reports back to the construction of pre-Muslim rammed earth sites in Spain lacking putlog
45 holes [4]. Modern rammed earth constructions often resort to externally supported formworks, but the shutters of
46 the later cover the entire wall (continuous formwork) and they are mainly composed by metallic elements, which
47 are stronger, stiffer and more durable than those made of timber. In this case, the compaction layers can be
48 extended through the full length of the wall.

49 Rammed earth construction has a long tradition in Portugal, where it prospered during the Islamic occupation of
50 the Iberian Peninsula between the 8th and 13th centuries, as evidenced by the still existing castles of Paderne and
51 Silves [6]. These fortifications are part of the military rammed earth built heritage and their walls are
52 characterised by large thickness (the thickness of Paderne's castle walls is of about 1.80 m) and high percentage
53 of stabilisation with lime [7], explaining their enhanced durability against weathering. Nevertheless, the
54 Portuguese rammed earth built stock is mainly constituted by civil constructions in the form of dwellings,
55 windmills, farm storehouses and churches [8]. Most of the existing dwellings were built until the 1950's and are
56 located in the southern regions of the country, namely in Alentejo, Algarve and Ribatejo [9].

57 The vernacular rammed earth dwellings from Alentejo are characterised by several features that vary from place
58 to place, according to the available resources, social and cultural factors [10]. Correia [9] performed a detailed in

59 situ survey that allowed to identify a series of architectonic and constructive features. In terms of geometry,
60 rammed earth buildings present in-plan rectangular shapes and are mainly constituted by a single storey,
61 although some cases of buildings in urban environment can present a second storey. In general, the facades
62 present few openings with small size, where the main facade presents a single door. The surfaces of the walls are
63 in general protected by means of mortar coatings consolidated by limeswash, which is yearly renewed [11].
64 Rammed earth walls are composed by blocks with 1.40-2.50 m length and 0.40-0.55 m height, compacted on
65 stone masonry plinths or directly on the ground. The thickness of the walls varies between 0.40 m and 0.57 m,
66 but in general is of about 0.50 m. Partition walls can be built in adobe or “*tabique*” (technique similar to wattle-
67 and-daub) and present slimmer thickness, namely 0.1-0.3 m. The soils used in the construction present a large
68 diversity according to the characteristics of the local soils, which can be differentiated in terms of colour (red,
69 yellow or grey), clay content (8-26%) and lithology (calcareous, quarzitic, sandstone and schist) [9][12][13]. In
70 general, rammed earth buildings present lightweight shed or gable roofs made of timber, where the rafters are
71 supported directly on the walls.

72 Building with rammed earth fell into disuse in Alentejo after the 1950’s, as a consequence of the growing use of
73 modern building materials (concrete, steel and fired bricks) and of the rural exodus of the populations [9].
74 However, the use of this technique was reborn in the 1980’s, driven initially by the need of conservation and
75 rehabilitation of the existing constructions [14]. The fact is that three decades of absence of new constructions in
76 rammed earth required relearning the technique, whose process was not an easy task since this traditional
77 knowledge became almost lost in time. This process was led by architects mesmerised by the technique, whose
78 inspiration was based on the teachings of the few living master builders (“*mestres taipeiros*”) [14].

79 Current rammed earth construction in Alentejo still keeps its traditional and vernacular roots, however a
80 paradigm shift is being introduced by a new generation of architects. Their inspiration starts putting aside the
81 original roots of rammed earth dwellings, and looks for a more daring architecture, driven by the particular
82 aesthetics of rammed earth walls and by an enhanced sustainable value. Thus, several changes are being
83 introduced both at the architectonic and technological levels, such as: (i) design of more complex plans,
84 elevations, roof systems and wall shapes; (ii) combination with modern materials (e.g. concrete and steel) (iii)
85 use of cement stabilised rammed earth; (iv) use of mechanised and heavier compaction systems (e.g. pneumatic
86 rammers and externally supported continuous formworks); (v) absence of protective plasters; (vi) surface
87 consolidation with silicate based products. Such changes are in line with industrialised rammed earth architecture

88 from other regions of the world, namely from the United States of America (USA), where this technique has
89 been used in the construction of luxurious houses and public buildings [15].

90 Building with raw earth brings many associated advantages (e.g. low initial embodied energy, adequate thermal
91 and acoustic performances, good fire resistance and enhanced indoor environment) [2][3][16], however earthen
92 structures show high seismic vulnerability [17][18], as evidenced by recent intense and destructive earthquakes
93 (e.g. Bam 2001, Pisco 2007 and Maule 2010). The high seismic vulnerability of these constructions is a
94 consequence of several factors, among which the poor connection between structural elements, high self-weight
95 and low mechanical properties are systematically the most highlighted. Recent research has been done to
96 characterise the experimental and numerical in-plane behaviour of rammed earth walls by means of diagonal
97 compression tests on wallets [8][19] and cyclic shear-compression tests on walls [20][21][22]. On the other
98 hand, the characterization of the out-of-plane behaviour of rammed earth is lacking in the literature and it is
99 resumed to a single research work [17], where overturning tests on walls and shaking table tests on small-scale
100 models were performed. In general, rammed earth was found to present high variability in terms of mechanical
101 properties and high non-linear mechanical behaviour, which has been object of recent numerical modelling using
102 the finite element method (FEM) [23][24] and the discrete element method (DEM) [25]. FEM was also used to
103 simulate the global seismic response of rammed earth buildings, namely by means of linear dynamic analyses
104 [26], pushover analyses [27] and non-linear dynamic analyses [28]. Nevertheless, these models were not
105 properly validated, because the proper characterisation of the dynamic behaviour of rammed earth structures is
106 lacking in the literature [29].

107 The seismic behaviour of rammed earth dwellings is still insufficiently comprehended, constituting a matter of
108 concern, namely in the case of southern Portugal. Here, Alentejo region is characterised by a moderate seismic
109 hazard, where the reference ground acceleration can achieve up to 2.0 m/s^2 [30]. Thus, assessing the seismic
110 performance of rammed earth structures is a topic requiring urgent investigation in order to promote the
111 protection of the existing vernacular heritage and the safety of modern constructions.

112 This paper intends to contribute for a better comprehension of the seismic performance of rammed earth
113 structures from Portugal based on the evaluation of simplified indexes and on experimental testing. The first
114 approach was applied to twenty traditional rammed earth dwellings surveyed in past works, while the second one
115 was used for a case study consisting of a recently built modern rammed earth house. It should be noted that the
116 evaluation of the seismic behaviour of traditional buildings based on simplified indexes is justified by the need
117 of adopting a fast and simple method for analysing and screening a large sample. Furthermore, the regular

118 geometry of these buildings is expected to result in a relatively reliable evaluation, in contrast with the much
119 more complex geometry of modern rammed earth structures. In this last case, a reliable evaluation must use
120 more sophisticated tools, such as material and structural characterisation through destructive and non-destructive
121 testing and numerical analyses.

122

123 **2. SIMPLIFIED SEISMIC EVALUATION**

124 To obtain a better understanding on the seismic performance of the traditional rammed earth heritage from
125 southern Portugal, a sample of case study buildings collected in past surveys is here considered [9] **Erro! A**
126 **origem da referência não foi encontrada.** The analysis of these buildings was performed based on the
127 evaluation of simplified indexes, following the approach proposed by Lourenço and Roque [32] and Lourenço et
128 al. [33]. These indexes are computed with basis on geometrical characteristics and on local seismic hazard, and
129 serve to provide a first screening approach to define a priority for further in-depth analysis.

130

131 **2.1 Methodology**

132 The use of simplified methods for seismic assessment is usually valid for masonry structures with “box-
133 behaviour” [34]. Ancient masonry structures, however, are usually disproved of rigid floors and present in-plane
134 shear and out-of-plane bending as dominant collapse modes. In general, traditional rammed earth dwellings can
135 hardly be considered as “box-behaviour” structures, since they are typically constituted by a single storey and by
136 a lightweight roof made of timber. Simplified methods cannot be assumed as valid approaches for quantitative
137 safety assessment of rammed earth buildings, nevertheless they can be used as qualitative indicators of their
138 relative seismic performance.

139 Four indexes were evaluated for each main direction (longitudinal X and transversal Y) of the investigated
140 rammed earth dwellings, namely three referring to in-plane failure (γ_1 , γ_2 and γ_3) and one to out-of-plane failure
141 (γ_λ).

142 Index γ_1 corresponds to the in-plan area ratio, as it results from the ratio between the area of the earthquake
143 resistant walls and the total in-plan area of the building:

$$\gamma_{1,i} = \frac{A_{wi}}{A_t} \quad [-] \quad \text{Eq. 1}$$

144

145 where A_{wi} is the area of the earthquake resistant walls in direction “ i ” and A_t is the total in-plan area of the
 146 building. Particular attention should be paid to the use of this index as it ignores the slenderness ratio of the walls
 147 and the mass of the building. In terms of threshold values for this index, Eurocode 8 [30] recommends values
 148 higher than 0.05-0.06 for regular structures with rigid floors. For cases where the design ground acceleration for
 149 rock-like soils is larger than 0.20g (high seismicity) a minimum value of 0.1 is recommended for historical
 150 masonry buildings [35]. In the case of rammed earth constructions, no threshold values are defined in the
 151 literature, whereby it was decided to use those proposed by Lourenço et al. [33] as merely indicative ones. Here,
 152 the threshold increases linearly with the peak ground acceleration (PGA).

153 Index γ_2 is the area to weight ratio, as it represents the ratio between the area of the earthquake resistant walls
 154 and the total weight of the building:

$$\gamma_{2,i} = \frac{A_{wi}}{G} \quad [L^2 F^{-1}] \quad \text{Eq. 2}$$

155
 156 where G is the quasi-permanent vertical action. Although, it takes into account the height of the building, this
 157 index presents the disadvantage of not being non-dimensional, meaning that it must be analysed for a fixed unit,
 158 which here is defined as m^2/MN . A minimum value of $1.2 m^2/MN$ is recommended for historical masonry
 159 buildings [35], but a more recent work [32] recommends a minimum value of $2.5 m^2/MN$ for high seismicity
 160 zones. Again, in the absence of any threshold for rammed earth constructions it was decided to use the same
 161 threshold proposed by Lourenço et al. [33], which increases linearly with the PGA value.

162 Index γ_3 corresponds to the base shear ratio and represents the ratio between the total shear for seismic loading
 163 (F_E) and the shear strength of the structure ($F_{Rd,i}$). The first parameter can be evaluated from an analysis with
 164 horizontal static loads equivalent to the seismic action ($F_E = \beta G$), where β is an equivalent seismic coefficient
 165 related to the design ground acceleration. The shear strength ($F_{Rd,i}$) can be estimated as the contribution of all
 166 earthquake resistant walls $F_{rd,i} = \sum A_{wi} f_{vk}$, where, according to Eurocode 6 [36], $f_{vk} = f_{vk0} + 0.4\sigma_d$. Here, f_{vk0} is the
 167 cohesion, which can be assumed equal to a low value or zero in the absence of further information, while 0.4
 168 corresponds to the tangent of the friction angle ($\tan \phi$). If f_{vk0} is assumed to be equal to zero for rammed earth, γ_3
 169 becomes independent from the building height and reads:

$$\gamma_{3,i} = \frac{A_{wi}}{A_w} \cdot \frac{\tan \phi}{\beta} \quad [-] \quad \text{Eq. 3}$$

170

171 where A_w is the total area of earthquake resistant walls and β is assumed to be equal to the PGA, as
 172 recommended by Lourenço et al. [33], due to the high difficulty and uncertainty in defining a more precise value.
 173 This index assumes a configuration similar to a traditional safety verification approach used for structural design,
 174 meaning that it must be higher than a threshold value of 1.

175 As for the out-of-plane index, γ_λ is the slenderness ratio between the height and thickness of the walls and reads:

$$\gamma_{\lambda,i} = \frac{h_{wi}}{t_w} \quad [-] \quad \text{Eq. 4}$$

176
 177 where h_{wi} is the height of the earthquake resistant walls subjected to out-of-plane loading in direction “ i ” and t_w
 178 is the thickness of the walls. In the case of this index, several references indicate possible maximum threshold
 179 values for earthen construction. NZS 4297 [37] is the most permissive by defining a threshold value of 10, while
 180 ASTM E2392-10 [38] is the most demanding one by defining a value of 6. Intermediate documents, such as
 181 Arya et al. [39], IS 13827 [40], NCB204 [41] and NMAC 14.7.4 [42], define a threshold value of 8.

182 The out-of-plane seismic performance of the traditional rammed earth dwellings from the case study sample was
 183 also evaluated by means of a kinematic approach [43][44] assuming a rigid rotating collapse mechanism. By
 184 considering horizontal forces proportional to mass and resorting to the virtual work principle, the capacity curve
 185 of a multi degree of freedom (MDOF) system in terms of displacement d and multiplier α can be obtained. The
 186 evaluation consists in comparing the seismic demand with the spectral acceleration of a single degree of freedom
 187 (SDOF) system equivalent to the MDOF system that activates the mechanism (here termed as a_0^*). Since the
 188 case study buildings consist of single storey structures, the system is a SDOF one. The centre of rotation was
 189 determined assuming no tensile strength and a compressive strength of 1.0 N/mm². It should be noted that a
 190 relatively low value of the compressive strength was assumed when compared with those reported by Miccoli et
 191 al. [19] for rammed earth. On the other hand, the assumed value is slightly lower than those (1.2-1.5 N/mm²)
 192 reported in research works dealing with the characterisation of unstabilised rammed earth from southern Portugal
 193 [8][45]. The seismic demand in the case of the linear kinematic analysis reads [44]:

$$Demand = \frac{a_g \cdot S}{q} \cdot \left(1 + 1.5 \frac{Z}{H} \right) \quad \text{Eq. 5}$$

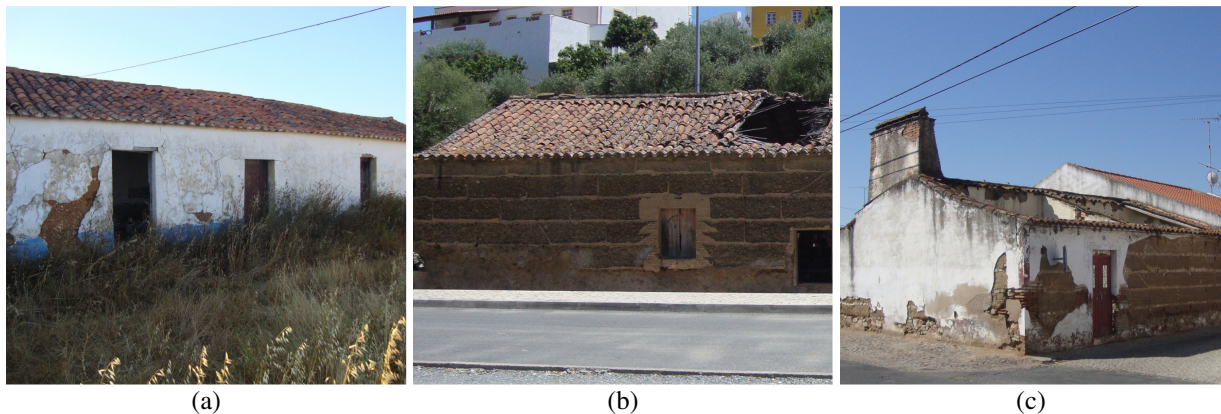
194
 195 where a_g is the PGA, q is a ductility factor, S is the type of soil, Z is the position of the centre of gravity and H is
 196 the height of the wall. For the analysis, a soil type C ($S = 1.20$) was selected as the worst likely case scenario
 197 provided by the national annex of Eurocode 8 [30]. The ductility factor was defined with basis on the Italian

198 code [44] by assuming that rammed earth behaves similarly to existing masonry structures, whose recommended
199 value is of 2.

200

201 **2.2 Surveyed buildings**

202 As stated previously, the sample of traditional rammed earth dwellings was obtained from past surveys carried
203 out in Alentejo (see Fig. 1), namely 9 buildings were studied by Domínguez [31] and 11 by Correia [9]. These
204 surveys collected a series of information from the buildings, namely location, current use, building materials
205 used, use of stone masonry plinths, number of storeys, surrounding environment, typology of the roof, use of
206 seismic retrofitting solutions and state of conservation. Nevertheless, the most relevant information regards plan
207 and elevation drafts with dimensions, which allowed to compute the indexes detailed in the previous section. The
208 identification of the construction date of the dwellings was not possible in most cases, yet it occurred before the
209 1950's. This fact means that their construction was not supported by any design project, further evidencing the
210 importance of conducting surveys to identify the features of this type of constructions in order to better
211 understand them.



212 Fig. 1 – Examples of analysed rammed earth buildings: (a) ID 1; (b) ID 5; (c) ID 8.

213

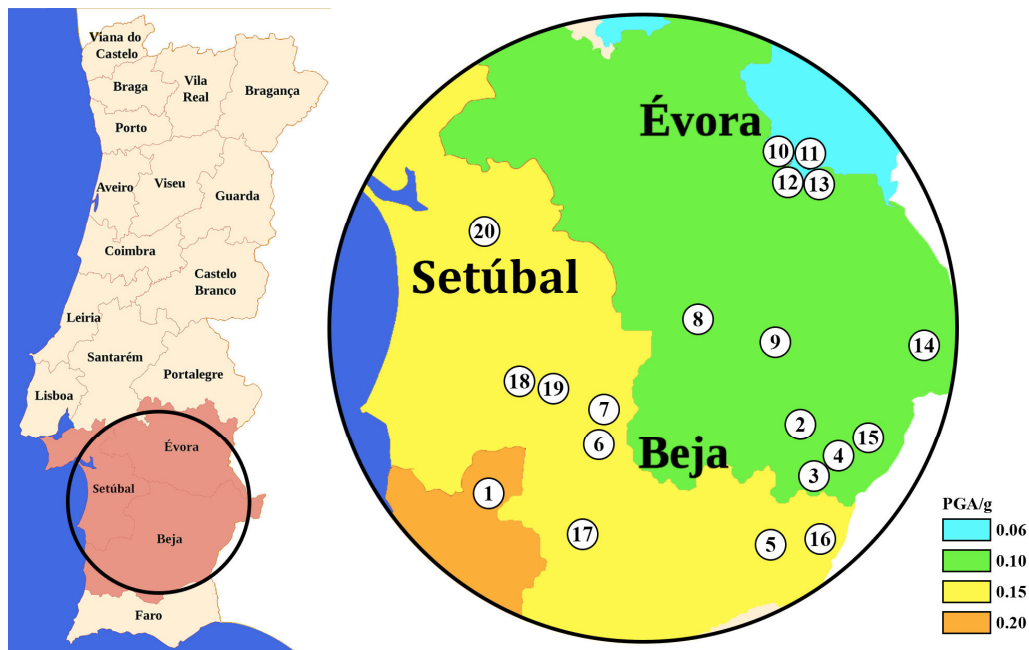
214 All rammed earth buildings of the sample are constituted by a single storey and their main characteristics are
215 presented in Table 1, namely in terms of typology of the roof, total in-plan area (A_t), longitudinal to transversal
216 length ratio (L/T), as well as average thickness (t_w) and height (h_w) of the walls. Furthermore, Fig. 2 illustrates
217 the location of the all dwellings of the sample and overlaps it with the seismic hazard zonation proposed in the
218 Portuguese national annex of Eurocode 8 [30] for far-field earthquakes. Adopting a far-field seismic action was
219 preferred over the near-field, since it presents higher spectral accelerations for larger period ranges, thus
220 representing the worst case scenario. The PGA considered for each of the dwellings is also given in Table 1.

221

Table 1 – Main characteristics of the traditional rammed earth dwellings in the case study sample.

ID	Ref.	Use	Location	Roof	PGA (g)	A_t (m ²)	L/T (-)	t_w (m)	h_w (m)
1	[31]	House	Colos	Gable	0.20	117	4.7	0.54	3.4
2	[31]	House	Serpa	Gable	0.10	149	1.6	0.54	2.9
3	[31]	House	Vales Mortos	Gable	0.10	236	2.9	0.58	3.3
4	[31]	House	Vales Mortos	Gable	0.10	146	1.3	0.50	2.5
5	[31]	House	Mértola	Gable	0.15	169	2.8	0.58	3.4
6	[31]	House	Aljustrel	Gable	0.15	65	1.1	0.52	2.9
7	[31]	House	Montes Velhos	Gable	0.10	96	1.6	0.50	3.0
8	[31]	House	Cuba	Gable	0.10	82	1.2	0.50	3.6
9	[31]	Farm	Pedrogão	Gable	0.10	250	4.4	0.50	3.3
10	[9]	Cellar	Montoito	Gable	0.06	130	3.2	0.54	3.1
11	[9]	Warehouse	Montoito	Gable	0.06	30	2.1	0.47	2.7
12	[9]	Warehouse	Montoito	Shed	0.06	40	2.0	0.50	2.9
13	[9]	House	Montoito	Gable	0.06	40	1.9	0.50	2.5
14	[9]	House	Safara	Shed	0.10	35	3.1	0.50	2.9
15	[9]	House	Vila Nova de S. Bento	Gable	0.10	85	1.7	0.46	2.4
16	[9]	House	Santana de Cambas	Gable	0.10	75	1.5	0.55	3.2
17	[9]	Corral	Saraiva	Gable	0.15	52	1.1	0.45	2.1
18	[9]	House	Ermidas-Sado	Gable	0.15	82	1.8	0.45	2.6
19	[9]	House	Ermidas-Sado	Gable	0.15	60	1.3	0.50	2.8
20	[9]	House	S. Maria do Castelo	Gable	0.15	67	4.3	0.50	2.9

223



224

225 Fig. 2 – Location of the rammed earth dwellings of the sample and comparison against the seismic hazard for
 226 far-field earthquakes.

227

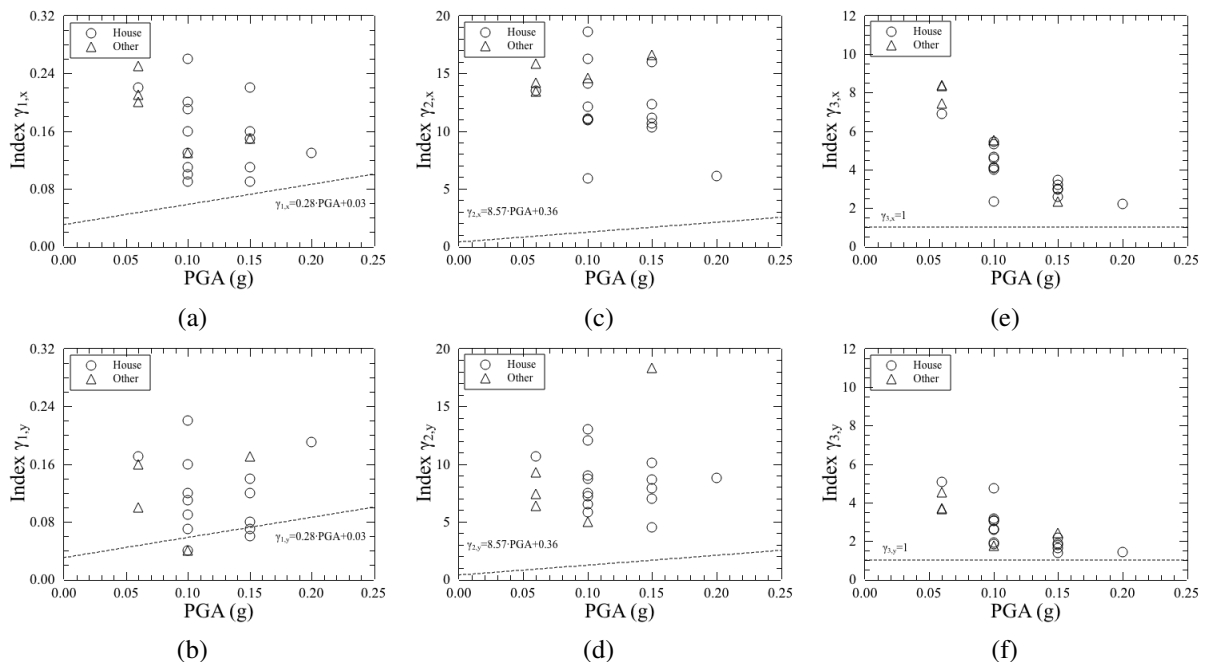
228 2.3 Results and analysis

229 To compute the simplified indexes, the density of the rammed earth was assumed as 1900 kg/m³, corresponding
 230 to an intermediate value of this property [19], whose variation may be beneficial or detrimental depending on the

231 index. The value of $\tan \phi$ involves high uncertainty in its estimation, whereby it was decided to adopt the
 232 minimum value presented by Jaquin et al. [46], namely 0.70 ($\phi = 35^\circ$).

233 The in-plane indexes obtained for all buildings, according to their main directions, are presented in Fig. 3 and are
 234 compared with the threshold values referred in Section 2.1. In general, the values of the indexes in the
 235 longitudinal direction (X) are higher than those in the transversal direction (Y), as a result of the rectangular plan
 236 development of this type of constructions. In fact, most of the resisting walls area in these buildings is positioned
 237 according to the longitudinal direction, indicating a potential better in-plane seismic response in this direction.
 238 The values obtained for γ_1 are located above the threshold, except for four buildings in the transversal direction
 239 (Y). In the case of γ_2 and γ_3 , the threshold is not violated in any direction. Furthermore, γ_3 is shown to be an
 240 index depending greatly on the local PGA, as the index value shows a clear decrease with the PGA increase.
 241 This situation seems to indicate that the in-plane seismic performance of traditional rammed earth constructions
 242 is compromised only in areas with high to very high seismic hazard (PGA above 0.2g). Furthermore, the
 243 decrease of index γ_3 with PGA increase and apparent random variation of indexes γ_1 and γ_2 with the PGA seem
 244 to indicate that no apparent correlation can be found between the local seismicity and the geometry of the
 245 dwellings.

246

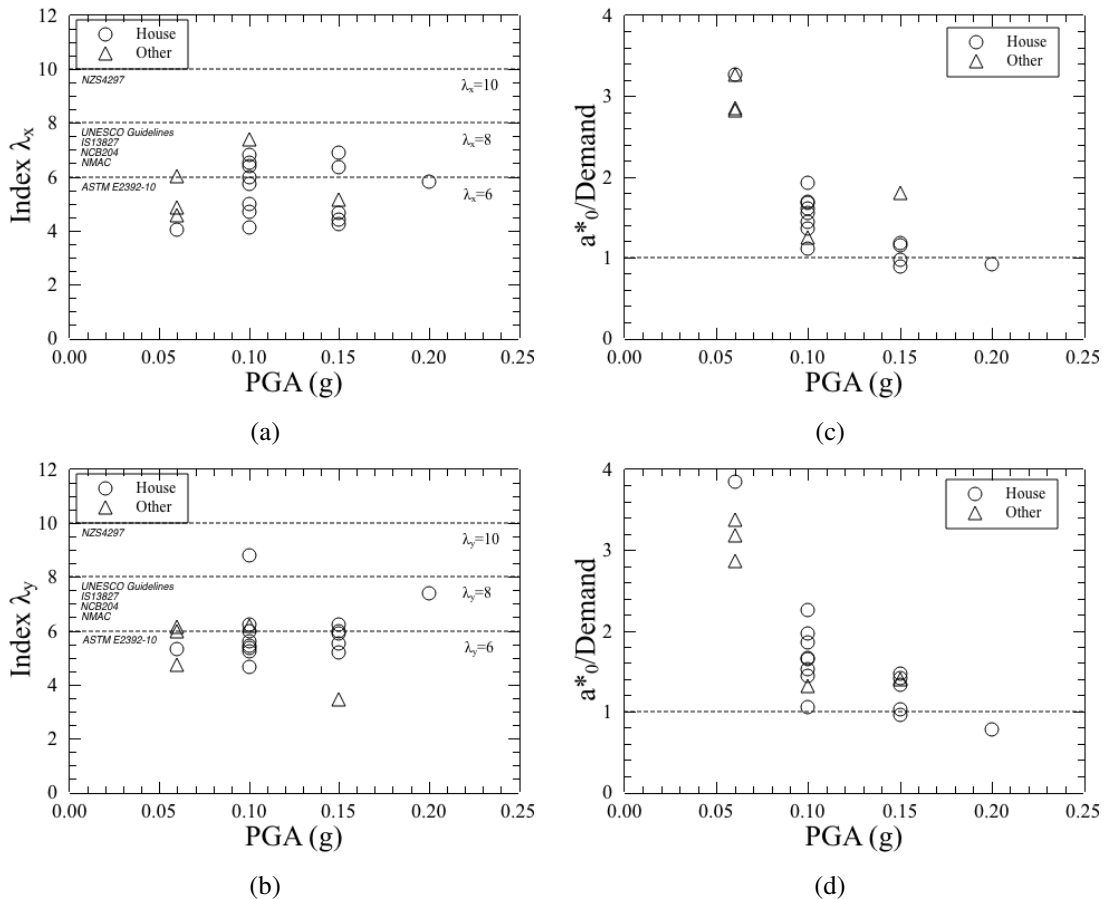


247 Fig. 3 – In-plane analysis of the buildings by index: (a) $\gamma_{1,x}$; (b) $\gamma_{1,y}$; (c) $\gamma_{2,x}$; (d) $\gamma_{2,y}$; (e) $\gamma_{3,x}$; (f) $\gamma_{3,y}$.

248

249 Fig. 4 presents the results of the out-plane analysis in terms of the index γ_λ and the kinematic approach
 250 verification. With respect to γ_λ , all buildings comply with the most permissive threshold and almost all buildings

251 comply with the intermediate threshold, with the exception of one case in the Y direction. However, the most
 252 demanding threshold is violated by 8 and by 5 buildings in X and Y directions, respectively. It should be noted
 253 that direction X is the most critical, since in most cases the height of the out-of-plane resisting walls is amplified
 254 due to the presence of gable walls. Also in the case of this index no apparent trend is observed with respect to
 255 the PGA, which seems to indicate that the different seismicity of the region had no influence on the definition of
 256 the geometry of the dwellings studied.



257 Fig. 4 – Out-of-plane analysis of the buildings: (a) $\lambda_{\lambda,x}$; (b) $\lambda_{\lambda,y}$; (c) kinematic approach in direction X; (d)
 258 kinematic approach in direction Y.

259
 260 With respect to the kinematic approach, the results outline a decreasing trend of the out-of-plane safety with
 261 increasing PGA, as expected. Nevertheless, it should be noted that the seismic capacity satisfies the seismic
 262 demand (threshold equal to 1) in almost all the cases, except for three buildings in the zones with PGA between
 263 0.15g and 0.20g. Furthermore, the seismic capacity of some buildings can be up to 1.5-4 times higher than the
 264 seismic demand for PGA lower than 0.15g.

265 In general, it can be stated that the capacity of most of the analysed buildings in satisfying the defined thresholds
 266 results from the use of traditional construction practices, namely the use of rectangular and regular plans, as well

267 as the use of very thick and low height rammed earth walls. In fact, it was observed that the height of the walls
268 was the characteristic presenting the highest variation among the buildings, whose importance can be assumed to
269 be high for the seismic performance of traditional rammed earth constructions. For instance, rammed earth
270 dwellings built to be used as low rise warehouses tend to be safer than houses, since fulfilling living conditions
271 required adopting taller walls.

272

273 **3. ADVANCED SEISMIC EVALUATION**

274 Modern rammed earth buildings can present complex structural systems, as consequence of adopting irregular
275 geometries (in-plan and elevation) and openings with unusual size and distribution, as well as of the
276 ineffectiveness of the connections between different structural elements (in particular those made with different
277 materials) and of the high non-linear behaviour of the rammed earth material. In general, the modelling of such
278 structures can be achieved by adopting advanced FEM models incorporating non-linear material behaviour and
279 time history analysis, which constitute time-demanding approaches, despite their high reliability. Nevertheless,
280 using such models requires knowing the material behaviour of the rammed earth and the dynamic properties of
281 the structure in detail.

282

283 **3.1 Methodology**

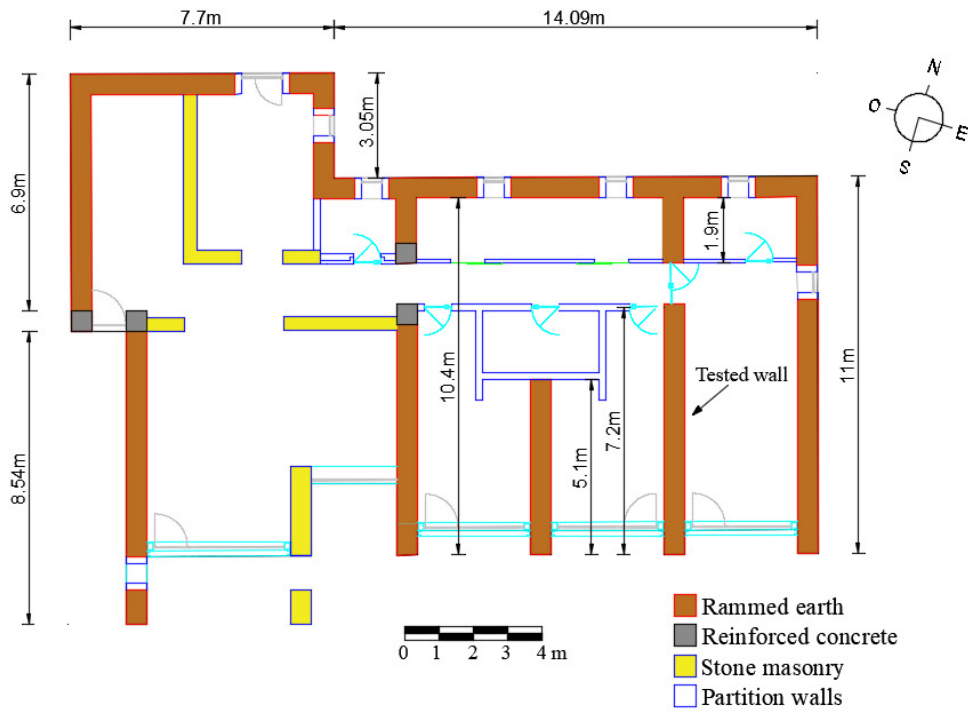
284 The material behaviour of rammed earth and the dynamic properties of the structure are adequately determined
285 by means of testing, following both destructive and non-destructive approaches. Within this context, this section
286 presents an experimental program aiming at characterising the mechanical and dynamic properties of the
287 rammed earth from a modern construction used as case study. The destructive approach included the execution
288 of compression tests on representative rammed earth specimens manufactured during the construction of the
289 walls. The non-destructive approach included the execution of sonic tests and dynamic identification tests on a
290 selected rammed earth wall of the case study. Furthermore, the subsequent analysis of the results through model
291 updating addressed the identification of material specificities affecting the dynamic response of rammed earth
292 structures, constituting a great contribute for the topic, given the general lack of investigation done so far. The
293 subsequent structural modelling and safety assessment of the whole structure is not addressed in this work, as the
294 focus of this research was on the use of advanced approaches able to provide suitable inputs to the
295 aforementioned FEM-based models.

296

297 **3.2 Description of the case study**

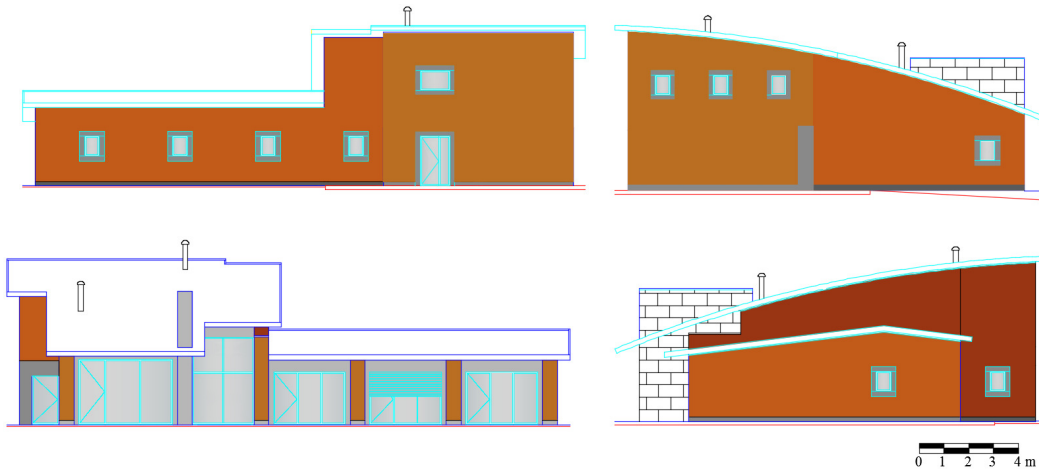
298 The case study consists of a private modern rammed earth house being built in Esposende, northern Portugal. It
299 should be noted that traditional houses from this region are mainly built with stone masonry, while reinforced
300 concrete (RC) framed structures with brick masonry infill dominate as building solution of modern houses [10].
301 Despite rammed earth construction has almost no tradition in northern Portugal, there are few reported cases,
302 namely in the nearby municipality of Viana do Castelo [47].

303 The house has an implantation area of about 230 m² (Fig. 5) and a maximum height of about 6.60 m (see Fig. 6),
304 allowing inclosing a second storey. The vertical structure consists mainly of rammed earth walls with 0.60 m
305 thickness, built on RC beams embedded in a foundation RC slab (Fig. 8a). The structure also includes additional
306 granite stone masonry walls and vertical steel elements, which are mainly used to support the second storey,
307 independently from the rammed earth walls. The rammed earth walls are mainly distributed in the transversal
308 direction, while in the longitudinal direction it is highlighted the lack of shear walls at the southern façade. The
309 roof consists of sandwich insulation panels supported on a timber structure. Furthermore, the doors located in
310 rammed walls are reinforced by means of RC frames built before compaction, while the windows openings
311 consist of pre-fabricated granite frames. These frames were placed at the desired position inside the formwork,
312 which was externally supported by metallic elements, while the shutters consisted of timber boards covering the
313 entire development of the wall (Fig. 8b). The rammed earth walls were built by a company with a long
314 experience in building with this technique. Despite the continuous formwork used, the compaction was made by
315 blocks (as in traditional rammed earth) with a horizontal indentation (see Fig. 8c) and using pneumatic rammers.



316
 317 Fig. 5 – First storey plan of the house adopted as case study.

318

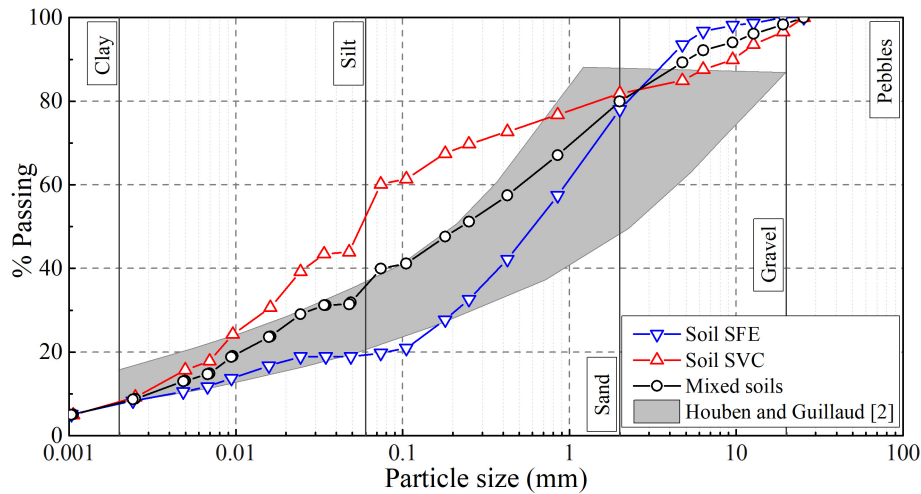


319
 320 Fig. 6 – Elevation views of the house adopted as case study.

321

322 The soil used in the construction of the rammed earth walls consists of a mixture of two other soils, namely a
 323 locally available soil (SFE) and a soil transported from a village located about 20 km away (SVC). SFE is a
 324 granitic residual soil with greyish colour, while SVC is a soil resulting from degradation of schist rock with
 325 brown-reddish colour. Both soils were characterised in terms of particle size distribution [48], consistency limits
 326 [49] and standard Proctor compaction [50]. The particle size distribution of the soils is presented in Fig. 7, while

327 Table 2 presents the liquid limit (LL), plastic limit (PL), plasticity index (PI), maximum dry density (γ_{dmax}) and
 328 optimum water content (W_{opt}).



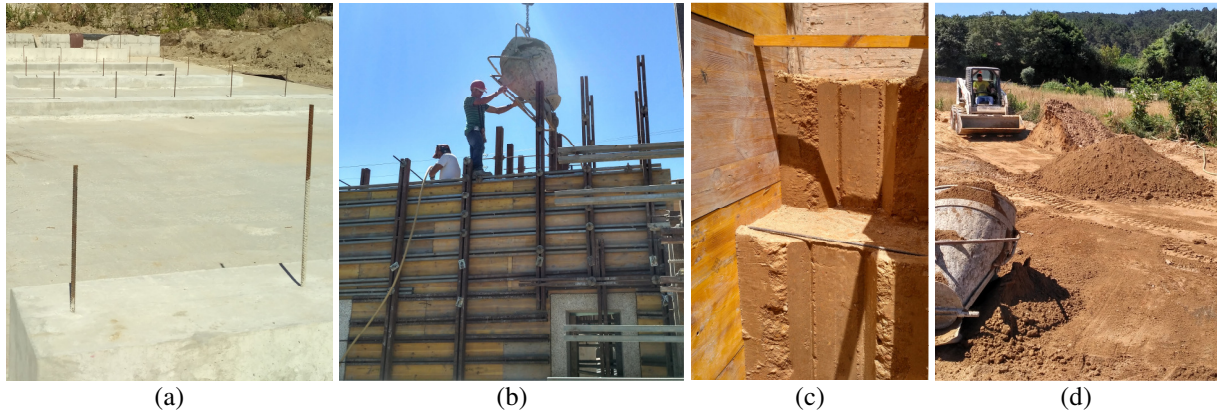
329
 330 Fig. 7 – Particle size distribution of the soils and comparison with the envelope proposed by Houben and
 331 Guillaud. [2].
 332

333 Table 2 – Properties of the soils.

Soil	LL (%)	PL (%)	PI (%)	γ_{dmax} (kg/m ³)	W_{opt} (%)
SFE		Non-plastic		2020	10.2
SVC		Non-plastic		1650	10.1

334
 335 Both soils present a clay content lower than 10%, which can be considered insufficient for unstabilised rammed
 336 earth construction, according to the envelope of suitable soils for rammed earth constructions proposed by
 337 Houben and Guillaud [2]. This observation means that using any of these soils for building rammed earth
 338 construction is expected to require introducing an additional amount of binder in order to promote adequate
 339 mechanical and durability characteristics. This enhancement can be achieved with chemical stabilisation, where
 340 cement is expected to be the most efficient binder for both soils, since they are deemed as non-plastic.
 341 Furthermore, the relatively high γ_{dmax} of soil SFE indicates that the resulting rammed earth is expected to present
 342 better mechanical performance than that of soil SVC. Despite the expected better performance of the local soil,
 343 the resulting aesthetics of the rammed earth was not as appealing as that of soil SVC, which results in rammed
 344 earth aesthetics similar to that of traditional rammed earth from Alentejo. Taking into account both mechanical
 345 performance and aesthetics preference criteria, the soil adopted for the construction of the walls resulted from the
 346 mixture of both soils in the proportion 1:1. The resulting mixed soil was stabilised by adding about 7% of
 347 Portland cement CEM II/B-L 32,5 N. The mixing of all constituents was processed mechanically, where water

348 was added using a hose and in proportions defined as adequate for compaction, according to the experience of
349 the workers (see Fig. 8d).



350 Fig. 8 – Construction of the rammed earth walls: (a) foundation RC beams; (b) externally supported formwork;
351 (c) horizontal indentation of the rammed earth blocks; (d) preparation of the soil mixture.

352

353 3.3 Destructive testing

354 The destructive testing approach consisted in compression tests performed on specimens' representative of the
355 rammed earth material of the walls. For this purpose, two sets of five specimens were sampled during the
356 construction of the walls, namely from two mixtures selected randomly. The specimens were compacted by the
357 workers while building the rammed earth walls, using cylindrical steel moulds (typically used for concrete
358 sampling) with 150 mm diameter and 300 mm height and a pneumatic compactor. The specimens were not
359 compacted in the full height of the mould due to limitations of the procedure (need of free space to introduce
360 loose soil mixture plus the compactor piston), meaning that the average height of the specimens was of about
361 230 mm (see Fig. 9a). After sampling, the moulds were covered with plastic and were moved to the Laboratory
362 of Structures from University of Minho (LEST), where they stayed under ambient conditions. Demoulding of the
363 specimens was processed at 7 days of age, which were then put to cure inside a climatic chamber with
364 temperature and relative humidity set as 20°C and 57.5%, respectively.



365 Fig. 9 – Compression tests: (a) sampling of the rammed earth specimens; (b) test setup.

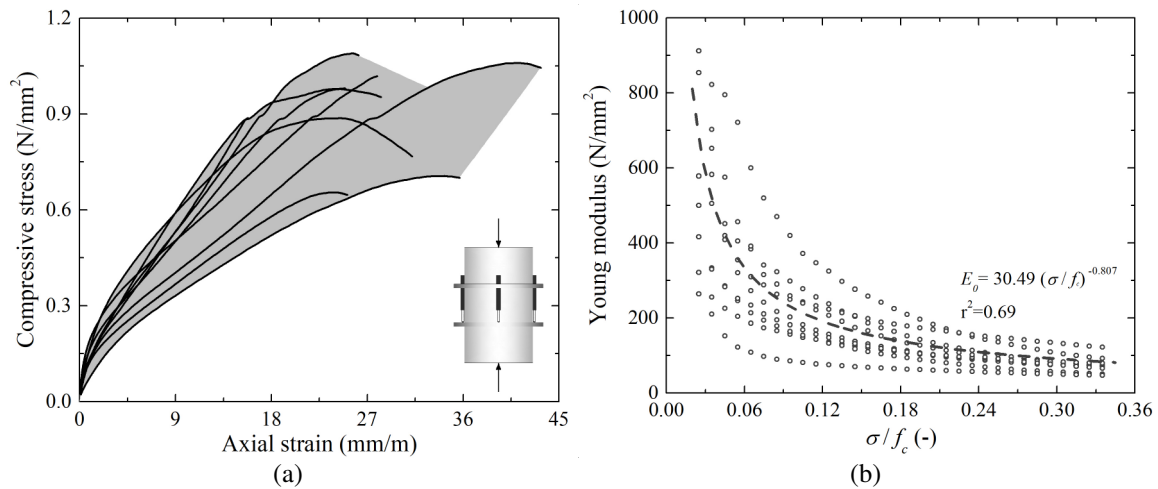
366 The specimens were tested with average age of about 32 days and density of about 1723 kg/m³ (CoV = 1.7%). In
367 the day before testing, the specimens were removed from the climatic chamber in order to regularise the loading
368 surfaces with fast hardening mortar. The compression tests were carried out under monotonic displacement
369 control with speed of 5 μm/s. The applied load was measured by means of a load cell, while the vertical
370 deformations at the middle third of each specimen were measured by means of three linear variable displacement
371 transducers (LVDT) radially-disposed (see Fig. 9b).

372 Fig. 10a presents the axial compressive stress-strain curves of the specimens of both sets, which evidence an
373 expressive scattering in terms of deformation behaviour. The average compressive strength of both sets of
374 specimens was of about 1.0 N/mm² (CoV = 16%), which is a value fitting within the range of values found in the
375 literature, namely 0.6-3.9 N/mm² [19].

376 The Young's modulus of each specimen was defined by linear fitting of the stress-strain curves at 5-30% of the
377 compressive strength, as proposed by Silva et al. [8], resulting in an average value of about 67 N/mm².
378 Nevertheless, the compressive stress-axial strain curves exhibit a pronounced non-linear behaviour during
379 loading, meaning that the Young's modulus depends on the stress level imposed to specimens, thus defining a
380 single value for this parameter seems to be a reckless procedure. This non-linear behaviour is clearly evidenced
381 in Fig. 10b, which presents the Young's modulus (secant modulus) of each specimen as function of the
382 compressive stress normalised by the compressive strength (σ/f_c). For low values of loading, the Young's
383 modulus assumes high values, which rapidly decrease (more than one order of magnitude) as the loading level
384 increases. Despite the high scattering of the results between specimens, this relationship seems to follow a power
385 law.

386 The fact is that insufficient discussion is available in the literature regarding the determination of the Young's
387 modulus of rammed earth materials by destructive means, namely with respect to the definition of the geometry
388 of the specimens, loading protocol and method to measure deformations. In general, rammed earth specimens
389 found in the literature [8][10][17][19][51] present very variable shapes (cubes, prisms, wallets, cylinders), the
390 loading protocols are found to be monotonic or with stepwise loading-unloading cycles, and the deformations are
391 monitored either by means of transducers measuring displacements between testing platens or of traducers fixed
392 directly on the specimen.

393



394 Fig. 10 – Results of the axial compression tests: (a) stress-strain curves; (b) variation of the Young's modulus
 395 with the compression level.

396

397 3.4 Non-destructive testing

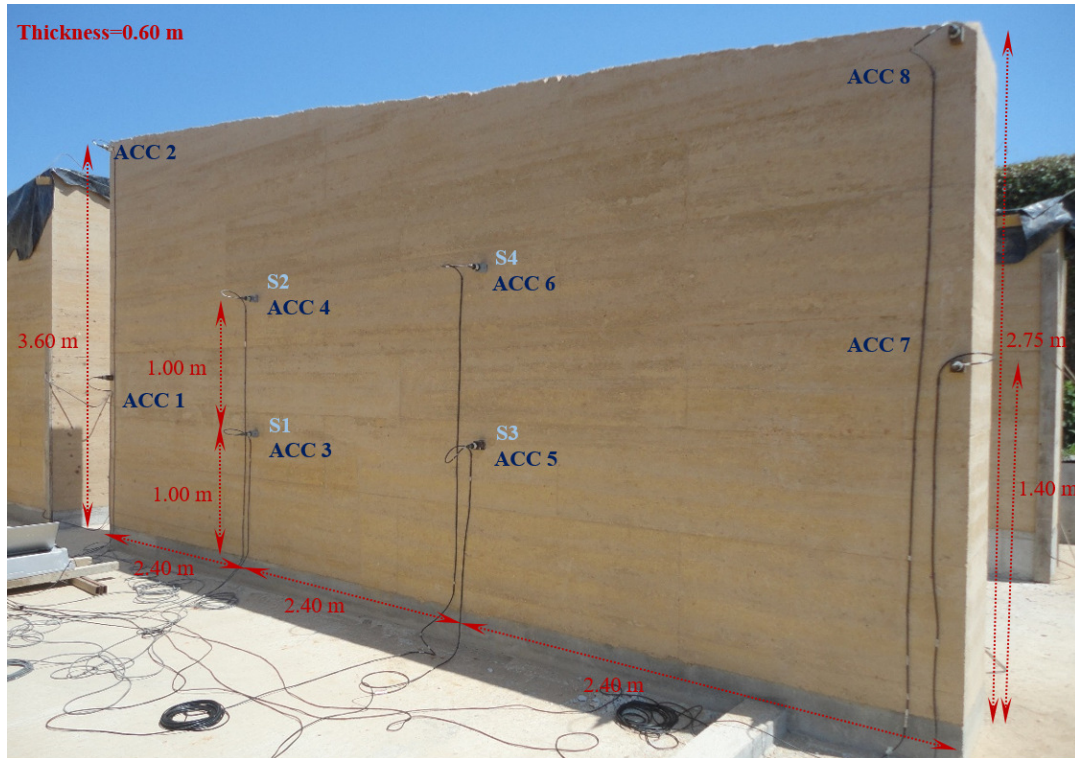
398 3.4.1 General description of the tests

399 An experimental in-situ campaign on a rammed earth wall of the case study described in Section 3.2 was carried
 400 out 27 days after compaction (see also Fig. 5). This experimental campaign involved two types of non-
 401 destructive tests, namely sonic tests and a dynamic identification test. Both types of tests aimed at estimating the
 402 dynamic Young's modulus of the rammed earth and the dynamic properties of the wall (frequencies, mode
 403 shapes and damping ratios).

404 The rammed earth wall includes a RC beam at its base (Fig. 11), connected to each other by means of vertical
 405 steel rebars (see Fig. 8a). All the other wall edges do not present any boundary condition and are free to deform.
 406 The rammed earth wall has a length of 7.20 m and variable height (maximum and minimum equal to 3.60 m and
 407 2.75 m, respectively). The thickness of the wall is constant and equal to 0.60 m (slenderness of about 5.3). The
 408 RC beam has 0.20 m high and the width is equal to the thickness of the wall.

409 In the non-destructive testing, piezoelectric accelerometers (sensitivity equal to 10 V/g, frequency range from
 410 0.15 to 1000 Hz, dynamic range $\pm 0.5g$, 210 gram weight), coaxial cables and one 24 bits data acquisition board
 411 with software developed by University of Minho were used. The accelerometers were fixed to timber cubes with
 412 screws. The timber cubes were glued to the wall with a small amount of fast-acting adhesive. Furthermore, an
 413 instrumented hammer (22240 N pk) was used for the sonic tests.

414



415

416 Fig. 11 – Rammed earth wall adopted for the non-destructive testing. (ACC_i and S_i correspond to the location of
 417 accelerometers used for dynamic identification tests and sonic tests, respectively)

418 *3.4.2 Sonic tests*

419 Direct sonic tests were carried out in four points (S1-S4) at the middle of the rammed earth wall (Fig. 11). The
 420 velocity of the P waves (V_p) in direct tests can be obtained by estimating the time (Δt) between the hammer
 421 impact and the arrival of the waves (signal of the accelerometer), and by knowing the thickness of the element
 422 (s) (Eq. 6):

$$V_p = \frac{s}{\Delta t} \quad \text{Eq. 6}$$

423

424 The dynamic Young's modulus (E_d) can be determined as function of the velocity of the P waves (V_p) and reads
 425 [52]:

$$E_d = \rho V_p^2 \frac{(1+\nu)(1-2\nu)}{(1-\nu)} \quad \text{Eq. 7}$$

426

427 where ρ is the density and ν is the dynamic Poisson's ratio. In this case study, the density is equal to 1723 kg/m³
 428 and the s is equal to 0.6 m. A Poisson's ratio equal to 0.2 was adopted. Six tests were carried out at each of the
 429 four points of the wall. Table 3 presents the average results obtained in the direct sonic tests. The average of the

430 velocity and dynamic Young's modulus in the perpendicular direction of the wall (in-plane direction of the
 431 layers) is equal to 544 m/s and 462 N/mm², respectively. Giamello et al. [53] carried out direct sonic tests on a
 432 rammed earth wall of an ancient Italian building and obtained an average velocity equal to 542 m/s, which is a
 433 value similar to that obtained here. Furthermore, the dynamic Young's modulus is found to be of about one order
 434 of magnitude higher than the Young's modulus reported from the compression tests. This large difference results
 435 from the fact that these parameters were evaluated accounting different stress levels, as discussed later.

436

437 Table 3 – Average of the results obtained in the direct sonic tests (CoV inside parenthesis).

	S1	S2	S3	S4	Average
V_P [m/s]	554.6 (7%)	537.5 (6%)	574.9 (10%)	509.4 (5%)	544.1 (5%)
E_d [N/mm ²]	479.2 (15%)	449.4 (12%)	516.9 (20%)	403.3 (10%)	462.2 (10%)

438

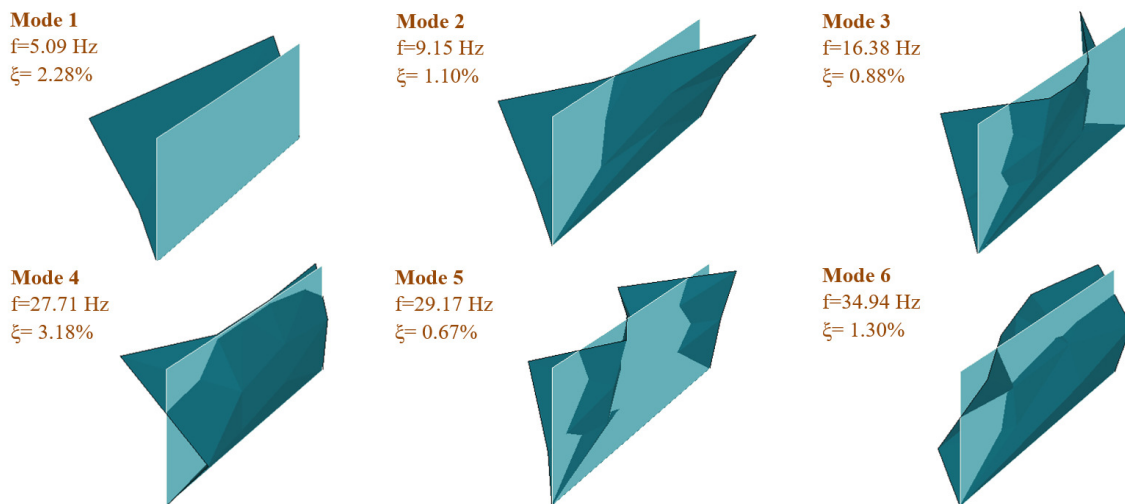
439 3.4.3 Dynamic identification test

440 The dynamic identification tests aim at estimating the dynamic properties, namely the frequencies, mode shapes
 441 and damping ratios of structures. The experimental modal identification techniques can be divided in three main
 442 groups [54]: (a) Input/output vibration tests, where the excitation applied to the structure and the vibration
 443 response are measured; (b) Output only vibration tests, where only the vibration response is measured during the
 444 service conditions of the structure; (c) Free vibration tests, where the structure is forced to an initial deformation
 445 and is then quickly released. Furthermore, several methods can be used to identify the dynamic properties
 446 through vibration tests, such as the Peak Picking, Circle Fit, Rational Fraction Polynomial or Complex
 447 Exponential. These methods are classified according the type of domain (frequency or time), the type of
 448 formulation (indirect or direct), the type of estimates (global or local), the number of the degrees of freedom
 449 (SDF - Single Degree of Freedom or MDF - Multiple Degree of Freedom), and the number of the input/output
 450 signals (SISO - Single Input and Single Output; SIMO - Single Input and Multiple Output or MIMO- Multiple
 451 Input and Multiple Output). For further details about the methods see Edwins [55], Peeters and De Roeck [56]
 452 and Gentile and Saisi [57].

453 The output-only technique was adopted in the dynamic identification test carried out on the rammed earth wall,
 454 in which the ambient vibration was the source of excitation (such as wind and traffic). This test aimed to
 455 estimate the out-of-plane vibration modes of the wall. Eight accelerometers fixed at several levels were used for
 456 the instrumentation of the wall, see Fig. 11. The signals were acquired with a sampling frequency equal to
 457 200 Hz and a total duration of 30 min. The results were processed in the ARTeMIS software [58] and the SSI-

458 UPC (Stochastic Subspace Identification-Principal Component) method [59] was adopted for estimating the
459 dynamic properties of the wall.

460 The dynamic identification test allowed to estimate six out-of-plane experimental modes, with frequencies
461 ranging from 5.09 Hz to 34.94 Hz (Fig. 12). Mode 1 (5.09 Hz) corresponds to the first global bending mode with
462 first curvature in elevation. The second mode (9.15 Hz) is an in-plan distortional mode. Mode 3 (16.38 Hz)
463 corresponds to an in-plan bending mode. The fourth mode presents second curvature in elevation (25.32 Hz).
464 Mode 5 (29.17 Hz) corresponds to an in-plan mode with second curvature and mode 6 (34.94 Hz) is a combined
465 bending mode with second curvature both in-plan and in elevation. The average of the damping ratios is equal to
466 1.8%, in which the damping ratio of the first mode equals 2.3% (Fig. 12). It is noted that the damping ratio is a
467 very sensitive parameter and difficult to estimate experimentally [60]. Furthermore, low values are expected for
468 the damping ratios when ambient vibrations are used to excite structures [61].



469
470 Fig. 12 – Dynamic properties estimated from the dynamic identification test.

471 472 3.5 Model updating

473 A numerical model of the rammed earth wall was prepared based on FEM [62], using eight-node shell elements,
474 based on the Mindlin-Reissner theory, and assuming that the base of the wall was fixed. The numerical
475 modelling aimed to estimate the elastic properties of the rammed earth based on the calibration of the dynamic
476 properties. The density (1723 kg/m^3) was considered constant during the model updating. The calibration was
477 carried out based on the Douglas-Reid proposal [63].

478 In the first attempt of the calibration process, six frequencies were considered and isotropic behaviour was
479 assumed for the rammed earth material. The numerical frequencies presented high errors with respect to the

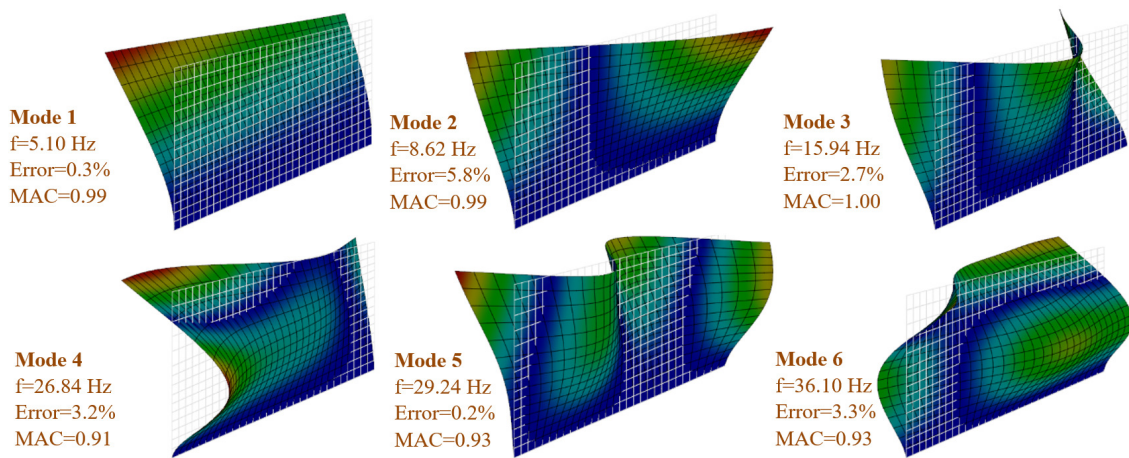
480 experimental ones (average and highest error equal to 12% and 22%, respectively). Furthermore, the sequence of
481 the numerical modes was not in agreement with that of the experimental ones. Thus, a comprehensive sensitivity
482 analysis was carried out, aiming at evaluating the parameters with influence on the dynamic properties of the
483 wall. The boundary conditions at the base (spring elements), the Poisson's ratio, the consideration of several
484 horizontal layers with different Young's modulus (isotropic behaviour) taking into account different compacting
485 energy, and the orthotropic (vertical direction and horizontal plan) behaviour of the material were evaluated. The
486 results of the sensitive analysis allowed to conclude that the orthotropic behaviour had the highest influence on
487 the dynamic properties. The Young's modulus in the vertical direction (i.e. perpendicular to layers) of the wall
488 (E_{\perp}) presents high influence on modes 1, 2, 4 and 6 (Fig. 12). In turn, the Young's modulus in the horizontal
489 direction (i.e. parallel to layers) of the wall (E_{\parallel}) has high influence on modes 3 and 5. Finally, the shear modulus
490 that relates the perpendicular and parallel directions ($G_{\perp\parallel}$) presents high influence on modes 2, 3 and 5.

491 In the final model updating of the model considering orthotropic behaviour, the three most important
492 uncorrelated variables, E_{\perp} , E_{\parallel} and $G_{\perp\parallel}$, were considered in the calibration process, whereas the Poisson's ratio in
493 the vertical direction (ν_{\perp}) and that in horizontal direction (ν_{\parallel}) were fixed as equal to ν (0.2). The shear modulus in
494 the plan of the layers ($G_{\parallel\parallel}$) was assumed equal to $E_{\parallel}/(2(1+\nu))$. It should be noted that despite the material
495 behaviour being assumed orthotropic, any value of E_{\parallel} evaluated in the direction perpendicular to the wall has no
496 influence on the dynamic properties estimated from the dynamic identification test. The calibrated model
497 presents an average error for the six frequencies less than 3% (Fig. 13 and Table 4), in which the error of the first
498 mode is equal to 0.3%. Furthermore, the average Modal Assurance Criteria (MAC) [59] is equal to 0.96 and the
499 MAC for the first mode equals 0.99 (Fig. 13), showing that the correlation between the numerical and
500 experimental mode shapes is very good. The calibrated properties (Table 4) obtained by the model updating are
501 equal to 515 N/mm², 998 N/mm² and 316 N/mm² for E_{\perp} , E_{\parallel} and $G_{\perp\parallel}$, respectively. Thus, $G_{\parallel\parallel}$ is computed as
502 416 N/mm². Now, if the equation $E/(2(1+\nu))$ is used for each direction, the shear modulus is equal to
503 215 N/mm² and 416 N/mm² for the directions perpendicular ($E_{\perp} = 515$ N/mm²) and parallel ($E_{\parallel} = 998$ N/mm²) to
504 the layers, respectively. The average value of these shear moduli is equal to 315 N/mm², which is approximately
505 equal to the shear modulus $G_{\perp\parallel}$ (316 N/mm²) obtained from the calibration assuming the variables as
506 uncorrelated.

507 The numerical modelling showed that an orthotropic behaviour should be considered for this case study. Bui and
508 Morel [51] carried out an experimental study on the anisotropy of rammed earth, in which the Young's moduli in
509 the perpendicular and parallel directions to the specimen's layers were determined for several amplitudes of

510 preloading. The results showed that for low levels of preloading (0.06 N/mm² to 0.12 N/mm²) the Young's
 511 modulus in the parallel direction to the layers ($E_{//}$) is higher than the Young's modulus in the parallel direction
 512 (E_{\perp}) for about 25%. However, for preloading equal to 0.40 N/mm² the difference is insignificant. In this case
 513 study, the compressive stress on the wall ranges from zero (top) to 0.06 N/mm² (base), thus a ratio between $E_{//}$
 514 and E_{\perp} higher than 1.25 should probably be expected. In fact, the $E_{//}$ to E_{\perp} ratio reaches 1.94. It is noted that the
 515 highest compressive stress in the wall is equal to 6% of the compressive strength of the rammed earth
 516 (Section 3.3).

517



518

519 Fig. 13 – Dynamic properties of the numerical model (only the modes estimated in the dynamic identification
 520 test are presented).

521

522 Table 4 – Experimental and numerical results obtained from the model updating.

Modes	Frequency			Material properties	Updated value
	Experimental [Hz]	Numerical [Hz]	Error [%]		
Mode 1	5.09	5.10	0.3%	E_{\perp} [N/mm ²]	515
Mode 2	9.15	8.62	-5.8%	$E_{//}$ [N/mm ²]	998
Mode 3	16.38	15.94	-2.7%	$G_{\perp//}$ [N/mm ²]	316
Mode 4	27.71	26.84	-3.2%	$G_{//}$ [N/mm ²]	416
Mode 5	29.17	29.24	0.2%	Density [kg/m ³]	1723
Mode 6	34.94	36.10	3.3%	Poisson's ratio	0.2

523

524 4. CONCLUSIONS

525 This paper presents an investigation that allows to better comprehend the seismic behaviour of rammed earth
 526 constructions from Portugal, by addressing both cases of traditional and modern constructions. Alentejo region
 527 was selected as case study for evaluating the seismic behaviour of a sample constituted by 20 traditional rammed
 528 earth dwellings, using simplified methods based on the analysis of in-plane and out-of-plane indexes, as well as
 529 by means of a kinematic approach. As for modern rammed earth construction, a rammed earth construction

530 recently built in Northern Portugal was used as case study, where factors affecting the seismic behaviour were
531 evaluated by means of destructive and non-destructive testing.

532 Despite the limitations of the simplified seismic evaluation carried out, it allowed to conclude that in general the
533 analysed dwellings are expected to perform reasonably well to a far-field earthquake. As for the in-plane
534 behaviour, four buildings (20%) violated γ_1 threshold, while none violated γ_2 or γ_3 . Nevertheless, it should be
535 noted that this conclusion results mainly from threshold values that were not defined specifically for rammed
536 earth constructions, thus the conclusions above must be taken with caution.

537 In the case of the out-of-plane behaviour, no building violated the most permissive threshold defined for γ_i ,
538 while only one building (5%) violated the intermediate threshold and 8 buildings (40%) violated the most
539 demanding threshold. The kinematic approach showed that only 3 buildings (15%) do not satisfy the demand
540 performance. Moreover, the longitudinal direction was shown to be the most critical due to the presence of gable
541 walls, which increase the height of the walls subjected to out-of-plane loading.

542 The advanced seismic evaluation consisted of destructive and non-destructive tests carried out within the
543 framework of the selected case study. The destructive testing involved a series of compression tests on
544 representative specimens, which mainly allowed to conclude that the compression behaviour of rammed earth is
545 highly non-linear. Furthermore, the Young's modulus of the rammed earth was shown to be highly dependent on
546 the stress level used for its evaluation.

547 The non-destructive tests involved carrying out sonic tests and a dynamic identification test on a rammed earth
548 wall from the case study. The sonic tests allowed to conclude that the dynamic Young's modulus in the
549 perpendicular direction to the wall (parallel to the layers) is equal to 462 N/mm². The dynamic identification
550 tests allowed to estimate the dynamic properties of the wall, namely six out-of-plane modes. Furthermore, a
551 numerical model was prepared and calibrated based on the dynamic properties estimated through the dynamic
552 identification test. The model updating presented an average error for the frequencies and MAC values of about
553 3% and 0.96, respectively. The calibration of the numerical model allowed also to conclude that rammed earth
554 should be considered as an orthotropic material for this case study, which presents low vertical loading and
555 several local modes. For walls subjected to higher stress levels (loaded slabs or heavy roofs at the top), the
556 influence of orthotropic behaviour of rammed earth would be probably less significant. The numerical Young's
557 modulus perpendicular to the layers is equal to 515 N/mm², which is significantly higher than the Young's
558 modulus computed between 5-30% of stress-strain curves (67 N/mm²). Nevertheless, when accounting for the
559 stress level of the walls at the middle section, the Young's modulus can be estimated from the destructive tests

560 (see equation in Fig. 10b) as 516-677 N/mm², which is a value relatively similar to that obtained from the model
561 updating. These aspects lead to the conclusion that the characterisation of the elastic properties of rammed earth
562 is still a challenge and more research should be conducted on this topic, namely in the study of the anisotropy
563 and the relationship between the static and dynamic Young's moduli.
564 Finally, it can be stated that the seismic behaviour of traditional rammed earth buildings from Alentejo benefits
565 from many features resulting from the local architectural culture, among which are the construction of buildings
566 with no more than a single storey (low rise buildings), with relatively regular plan and elevation and with very
567 thick walls. Nevertheless, modern rammed earth construction has been leading to increasingly more complex
568 structures, where some of the aforementioned features are neglected. Thus, the design of these structures in
569 regions with important seismic hazard requires using reliable design tools, capable of taking into account the key
570 factors affecting the seismic response. Here, the adequate determination of the mechanical properties of rammed
571 earth by means of experimental testing assumes a central role, but it was shown to be a topic needing further
572 research.

573

574 **ACKNOWLEDGEMENTS**

575 This work was partly financed by FEDER funds through the Competitivity Factors Operational Programme -
576 COMPETE and by national funds through FCT – Foundation for Science and Technology within the scope of
577 projects POCI-01-0145-FEDER-007633 and POCI-01-0145-FEDER-016737 (PTDC/ECM-EST/2777/2014).
578 The support from grant SFRH/BPD/97082/2013 is also acknowledged. The authors wish also to express
579 gratitude to Eng. Sérgio Morgado and Mr. Francisco Seixas for providing access to the house of Forjães and
580 conditions to perform the destructive and non-destructive tests.

581

582 **REFERENCES**

- 583 [1] Schroeder, H. (2016). The Development of Earth Building. In Sustainable Building with Earth. Springer
584 International Publishing, pp. 1-46.
- 585 [2] Houben H., Guillaud H. (2008) Earth Construction: A Comprehensive Guide. 3rd Edition, CRATerre -
586 EAG, Intermediate Technology Publication, London, UK.
- 587 [3] Minke G. (2006) Building with earth, design and technology of a sustainable architecture. Birkhäuser –
588 Publishers for Architecture, Basel- Berlin-Boston.

- 589 [4] Jaquin P.A. Analysis of Historic Rammed Earth Construction, PhD Thesis, Durham University, Durham,
590 United Kingdom, 2008.
- 591 [5] Silva R.A., Jaquin P.A., Oliveira D.V., Miranda T.F., Schueremans L., Cristelo N. (2014). Conservation
592 and new construction solutions in rammed earth. In Structural rehabilitation of old buildings (pp. 77-108).
593 Springer Berlin Heidelberg.
- 594 [6] Correia, M. Islamic fortresses in military rammed earth, *Pedra & Cal*, 24 (2004), pp. 16. (in Portuguese)
- 595 [7] Braga A.M., Estêvão J.M.C. (2010). The earthquakes and the rammed earth construction in Algarve. In
596 proc. of Congresso Nacional de Sismologia e Engenharia. SÍSMICA 2010, 20-23 October; Aveiro,
597 Portugal. (in Portuguese)
- 598 [8] Silva R.A., Oliveira D.V., Schueremans L., Miranda T., Machado J. (2016). Effectiveness of the repair of
599 unstabilised rammed earth with injection of mud grouts. *Construction and Building Materials*, 127, 861-
600 871.
- 601 [9] Correia M. (2007) *Rammed Earth in Alentejo*. Argumentum, Lisbon.
- 602 [10] Silva R.A., Oliveira D.V., Miranda T., Cristelo N., Escobar M.C., Soares E. (2013) Rammed earth
603 construction with granitic residual soils: The case study of northern Portugal, *Construction and Building*
604 *Materials*, 47, pp. 181-191.
- 605 [11] Gil M., Aguiar J., Seruya A., Veiga R., Carvalho L., Vargas H., Mirão J., Candeias A. (2011). Colour
606 Assays: an inside look into Alentejo traditional limewash paintings and coloured lime mortars. *Color*
607 *Research & Application*, 36(1), 61-71.
- 608 [12] Silva R.A. (2013). Repair of earth constructions by means of grout injection. PhD thesis, University of
609 Minho, Guimarães, Portugal.
- 610 [13] Gomes M.I., Gonçalves T.D., Faria P. (2014). Unstabilized rammed earth: characterization of material
611 collected from old constructions in south portugal and comparison to normative requirements. *International*
612 *Journal of Architectural Heritage*, 8(2), 185-212.
- 613 [14] Marques J., Lima P.A., Vale C.P. (2014). Contemporary use of rammed earth in Portugal. The case of
614 Alentejo coast. 40th IAHS World Congress on Housing - Sustainable Housing Construction, 16-19
615 December 2014, Funchal, Portugal.
- 616 [15] Lima P.A., Marques J., Vale, C.P. (2016). Rammed Earth Construction Nowadays-Comparing
617 Methodologies and Design Between Portugal and USA. 12th World Congress on Earthen Architecture
618 (TERRA 2016), 11-14 July 2016, Lyon, France.

- 619 [16] Allinson D, Hall M. (2012) Humidity buffering using stabilised rammed earth materials. In: Proceedings of
620 the ICE-Construction Materials, vol. 165(6), pp. 335-344.
- 621 [17] Yamín Lacouture L. E., Phillips Bernal C., Ortiz R., Carlos J., Ruiz Valencia D. (2007). Estudios de
622 vulnerabilidad sísmica, rehabilitación y refuerzo de casas en adobe y tapia pisada. Apuntes: Revista de
623 Estudios sobre Patrimonio Cultural-Journal of Cultural Heritage Studies, 20(2), 286-303.
- 624 [18] Oliveira D.V., Silva R.A., Lourenço P.B., Schueremans, L. (2010). As construções em taipa e os sismos. In
625 proc. of Congresso Nacional de Sismologia e Engenharia - SÍMICA 2010, Aveiro, 2010. (in Portuguese)
- 626 [19] Miccoli L., Müller U., Fontana P. (2014). Mechanical behaviour of earthen materials: a comparison
627 between earth block masonry, rammed earth and cob. Construction and Building Materials, 61, 327-339.
- 628 [20] Nabouch R., Bui Q.B., Plé O., Perrotin P., Poinard C., Goldin T., Plassiard J.P. (2016). Seismic Assessment
629 of Rammed Earth Walls Using Pushover Tests. Procedia Engineering, 145, 1185-1192.
- 630 [21] Miccoli L., Drougkas A., Müller U. (2016). In-plane behaviour of rammed earth under cyclic loading:
631 Experimental testing and finite element modelling. Engineering Structures, 125, 144-152.
- 632 [22] Arslan M.E., Emiroğlu M., Yalama A. (2017). Structural behavior of rammed earth walls under lateral
633 cyclic loading: A comparative experimental study. Construction and Building Materials, 133, 433-442.
- 634 [23] Silva R.A., Oliveira D.V., Schueremans L., Lourenço P.B., Miranda T. (2014). Modelling the structural
635 behaviour of rammed earth components. Proceedings of the 12th International Conference on
636 Computational Structures Technology, B.H.V. Topping and P. Iványi, (Editors), Civil-Comp Press,
637 Stirlingshire, Scotland.
- 638 [24] Miccoli L, Oliveira D.V., Silva R.A., Müller U., Schueremans L. (2015). Static behaviour of rammed earth:
639 experimental testing and finite element modelling. Materials and Structures, 48, 3443-3456.
- 640 [25] Bui, T. T., Bui, Q. B., Limam, A., Morel, J. C. (2015). Modeling rammed earth wall using discrete element
641 method. Continuum Mechanics and Thermodynamics, 28, 523-538.
- 642 [26] Gomes M.I., Lopes M., de Brito J. (2011). Seismic resistance of earth construction in Portugal. Engineering
643 Structures, 33(3), 932-941.
- 644 [27] Ortega J., Vasconcelos G., Correia M., Rodrigues H., Lourenço P.B., Varum H. (2015). Evaluation of
645 seismic vulnerability assessment parameters for Portuguese vernacular constructions with nonlinear
646 numerical analysis. COMPDYN 2015 5th ECCOMAS Thematic Conference on Computational Methods in
647 Structural Dynamics and Earthquake Engineering M. Papadrakakis, V. Papadopoulos, V. Plevris (eds.)
648 Crete Island, Greece, 25-27 May 2015.

- 649 [28] Librici C. (2016). Modelling of the seismic performance of a rammed earth building. MSc. thesis,
650 University of Minho, Guimarães.
- 651 [29] Bui Q.B., Hans S., Morel J.C., Do A.P. (2011). First exploratory study on dynamic characteristics of
652 rammed earth buildings. *Engineering Structures*, 33, 3690-3695.
- 653 [30] IPQ (2009). NP ENV 1998-1: Eurocode 8: Design of structures for earthquake resistance – Part 1: General
654 rules, seismic actions and rules for buildings. Instituto Português da Qualidade, Lisbon.
- 655 [31] Domínguez O. (2015). Preservation of rammed earth constructions. MSc thesis (SAHC), University of
656 Minho, Guimarães.
- 657 [32] Lourenço P.B., Roque J.A. (2006). Simplified indexes for the seismic vulnerability of ancient masonry
658 buildings. *Construction and Building Materials*, 20, 200-208.
- 659 [33] Lourenço P.B., Oliveira D.V., Leite J.C., Ingham J.M., Modena C., da Porto F. (2013). Simplified indexes
660 for the seismic assessment of masonry buildings: International database and validation. *Engineering Failure*
661 *Analysis*, 34, 585-605.
- 662 [34] Lourenço P.B., Mendes N., Ramos L.F., Oliveira D.V. (2011). Analysis of masonry structures without box
663 behavior. *International Journal Architectural Heritage*, 5, 369-382.
- 664 [35] Meli R. (1998). *Structural engineering of historical buildings*. Mexico-City: Fundación ICA; 1998 (in
665 Spanish).
- 666 [36] CEN (2005). EN 1996-1-1: Eurocode 6: Design of masonry structures, Part 1-1: General rules for
667 reinforced and unreinforced masonry structures. European Committee of Standardization. Brussels.
- 668 [37] NZS (1998). NZS 4297: Engineering design of earth buildings. Standards New Zealand: Wellington.
- 669 [38] ASTM (2010). ASTM E2392-10: Standard Guide for Design of Earthen Wall Building Systems. American
670 Society for Testing and Materials: West Conshohocken.
- 671 [39] Arya A.S., Boen T., Ishiyama Y. (2014). Guidelines for earthquake resistant non-engineered construction.
672 UNESCO.
- 673 [40] IS (1998) IS13827: Improving Earthquake Resistance of Earthen Buildings – Guidelines. Bureau of Indian
674 Standards: New Delhi.
- 675 [41] NNBC (1994). NBC204:1994 Guidelines for Earthquake Resistant Building Constructions: Earthen
676 Building. Government of Nepal, Ministry of Physical Planning and Works, Department of Urban
677 Development and Building Construction: Babar Mahal, Kathmandu, Nepal.

- 678 [42] NMAC (2004). NMAC 14.7.4: New Mexico Earthen Building Materials Code. NM: Construction
679 Industries Division (CID) of the Regulation and Licensing Department: Santa Fé.
- 680 [43] Mendes N. (2014). Masonry macro-block analysis. Encyclopedia of Earthquake Engineering. Eds. Beer M,
681 Kougoumtzoglou I.A., Patelli E., Siu-Kui Au I. Springer Berlin Heidelberg. (online)
- 682 [44] Consiglio Superiore dei Lavori Pubblici (2008). Nuove Norme Tecniche per le Costruzioni, D.M.
683 Infrastrutture 14/01/2008, published on S.O. no. 30 at the G.U. 04/02/2008 no. 29 (in Italian)
- 684 [45] Silva R.A., Domínguez-Martinez O., Oliveira D.V., Pereira E., Soares E. (2016). Assessment of the
685 injection of grouts to repair cracks in rammed earth. In proc. International RILEM Conference on
686 Materials, Systems and Structures in Civil Engineering, Conference segment on Historical Masonry, 22-24
687 August, Lyngby, Denmark.
- 688 [46] Jaquin P.A., Augarde C.E., Gerrard C.M. (2006). Analysis of historic rammed earth construction. In Proc.
689 5th Int. Conf. Structural Analysis of Historical Constructions, New Delhi, India, Vol. 2, 1091-1098.
- 690 [47] Correia M., Merten, J. (2005). A taipa alentejana: sistemas tradicionais de protecção. IVseminário ibero-
691 Americano de construção com terra e III seminário arquitectura de terra em Monsaraz, Portugal; 2005.
- 692 [48] LNEC (1966). LNEC E 196-1966 - Solos. Análise granulométrica. Laboratório Nacional de Engenharia
693 Civil, Lisbon. (in Portuguese)
- 694 [49] IPQ (1969). NP 143:1969 – Solos. Determinação dos limites de Consistência. Instituto Português da
695 Qualidade, Caparica. (in Portuguese)
- 696 [50] LNEC (1966). LNEC E 197-1966 - Solos. Ensaio de compactação. Laboratório Nacional de Engenharia
697 Civil, Lisbon. (in Portuguese)
- 698 [51] Bui Q., Morel J. (2009). Assessing the anisotropy of rammed earth. Construction and Building Materials,
699 23, 3005-3011. DOI: 10.1016/j.conbuildmat.2009.04.011
- 700 [52] BSI (1986). BS 1881-203: Testing concrete - Part 203: Recommendations for measurement of velocity of
701 ultrasonic pulses in concrete. British Standard, London.
- 702 [53] Giamello M., Fratini F., Mugnaini S., Pecchioni E., Droghini F., Gabbrielli F., Giorgi E., Manzoni E.,
703 Casarin F., Magrini A., Randazzo F. (2016). Earth masonries in Medieval Grange of Cuna - Siena (Italy).
704 Journal of Materials and Environmental Science, 7(10), 3509-3521.
- 705 [54] Ramos L.F. (2007). Damage identification on masonry structures based on vibration signatures. PhD
706 Thesis. University of Minho, Portugal. (<http://hdl.handle.net/1822/7380>)

- 707 [55] Ewins D. (2000). Modal testing: theory, practice and application. 2nd Edition, Research Studies Press LTD,
708 Baldock, Hertfordshire, England.
- 709 [56] Peeters B., De Roeck G. (1999). Reference-based stochastic subspace identification for output-only modal
710 analysis. *Mechanical Systems and Signal Processing*, 13, 6, 855-878.
- 711 [57] Gentile C., Saisi A. (2007). Ambient vibration testing of historic masonry towers for structural
712 identification and damage assessment. *Construction and Building Materials*, 21, 1311–1321.
- 713 [58] ARTeMIS (2013). Ambient Response Testing and Modal Identification Software. SVS - Structural
714 Vibration Solutions A/S. Modal 2.5. Denmark.
- 715 [59] Ewins D. (2000). Modal testing: theory, practice and application. Research Studies Press LTD, Baldock,
716 Hertfordshire, England.
- 717 [60] Mendes N. (2012). Seismic assessment of ancient masonry buildings: Shaking table tests and numerical
718 analysis. PhD Thesis, University of Minho, Portugal.
- 719 [61] Lourenço P.B., Trujilo A., Mendes N., Ramos L.F. (2012). Seismic performance of the St. George of the
720 Latins church: Lessons learned from studying masonry ruins. *Engineering Structures*, 40, 501-518. DOI:
721 10.1016/j.engstruct.2012.03.003.
- 722 [62] DIANA FEA BV (2017). DIplacement method ANAlyser. Release 10.1, Netherlands.
- 723 [63] Douglas B., Reid W. (1982). Dynamic tests and system identification of bridges. *Journal of the Structural*
724 *Division*, 108(10), 2295-2312.

725 **LIST OF TABLE CAPTIONS**

726

727 Table 1 – Main characteristics of the traditional rammed earth dwellings in the case study sample.

728 Table 2 – Properties of the soils.

729 Table 3 – Average of the results obtained in the direct sonic tests (CoV inside parenthesis).

730 Table 4 – Experimental and numerical results obtained from the model updating.

731

732

733 **LIST OF FIGURE CAPTIONS**

734

735 Fig. 1 – Examples of analysed rammed earth buildings: (a) ID 1; (b) ID 5; (c) ID 8.

736 Fig. 2 – Location of the rammed earth dwellings of the sample and comparison against the seismic hazard for
737 far-field earthquakes.

738 Fig. 3 – In-plane analysis of the buildings by index: (a) $\gamma_{1,X}$; (b) $\gamma_{1,Y}$; (c) $\gamma_{2,X}$; (d) $\gamma_{2,Y}$; (e) $\gamma_{3,X}$; (f) $\gamma_{3,Y}$.

739 Fig. 4 – Out-of-plane analysis of the buildings: (a) $\gamma_{\lambda,X}$; (b) $\gamma_{\lambda,Y}$; (c) kinematic approach in direction X; (d)
740 kinematic approach in direction Y.

741 Fig. 5 – First storey plan of the house adopted as case study.

742 Fig. 6 – Elevation views of the house adopted as case study.

743 Fig. 7 – Particle size distribution of the soils and comparison with the envelope proposed by Houben and
744 Guillaud. [2].

745 Fig. 8 – Construction of the rammed earth walls: (a) foundation RC beams; (b) externally supported formwork;
746 (c) horizontal indentation of the rammed earth blocks; (d) preparation of the soil mixture.

747 Fig. 9 – Compression tests: (a) sampling of the rammed earth specimens; (b) test setup.

748 Fig. 10 – Results of the axial compression tests: (a) stress-strain curves; (b) variation of the Young's modulus
749 with the compression level.

750 Fig. 11 – Rammed earth wall adopted for the non-destructive testing. (ACC_i and S_i correspond to the location of
751 accelerometers used for dynamic identification tests and sonic tests, respectively)

752 Fig. 12 – Dynamic properties estimated from the dynamic identification test.

753 Fig. 13 – Dynamic properties of the numerical model (only the modes estimated in the dynamic identification
754 test are presented).

755